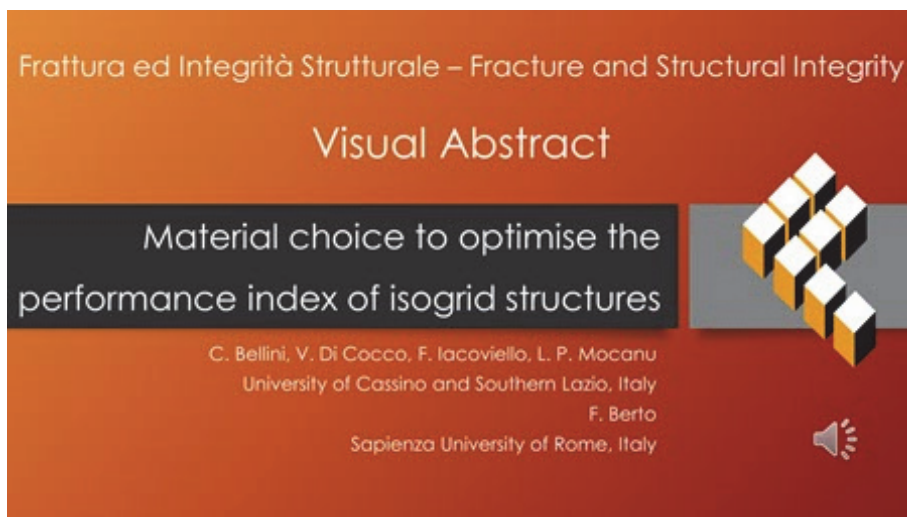




Material choice to optimise the performance index of isogrid structures

C. Bellini, V. Di Cocco, F. Iacoviello, L. P. Mocanu
University of Cassino and Southern Lazio, Italy
costanzo.bellini@unicas.it, <http://orcid.org/0000-0003-4804-6588>
vittorio.dicocco@unicas.it, <http://orcid.org/0000-0002-1668-3729>
francesco.iacoviello@unicas.it, <http://orcid.org/0000-0002-9382-6092>
larisapatricia.mocanu@unicas.it, <https://orcid.org/0000-0002-3432-9774>

F. Berto
Sapienza University of Rome, Italy
filippo.berto@uniroma1.it, <http://orcid.org/0000-0001-9676-9970>



Citation: Bellini, C., Berto, F., Di Cocco, V., Iacoviello, F., Mocanu, L. P., Material choice to optimise the performance index of isogrid structures, *Frattura ed Integrità Strutturale*, 67 (2024) 231-239.

Received: 03.11.2023
Accepted: 05.12.2023
Online first: 07.12.2023
Published: 01.01.2024

Copyright: © 2022 This is an open access article under the terms of the CC-BY 4.0, which permits unrestricted use, distribution, and reproduction in any medium, provided the original author and source are credited.

KEYWORDS. Carbon fibre, Titanium, Performance index, Finite element analysis, Isogrid.

INTRODUCTION

Thin constructions exposed to compressive loads frequently experience buckling phenomena; thus, designers must find a workable solution for this problem. The first way to solve this issue is to expand the structural element sections, but doing so increases weight, which could not be desirable for certain scenarios, particularly in the aviation industry [1]. Consequently, a better approach would be to use ribs adhered to the thin panels' surface to strengthen them



[2]. As it comes to isogrid structures, buckling is the most common type of failure. Depending on the structure geometric properties and the applied load, buckling can be either local or global. A rib may break in the former kind of buckling, whereas the latter involves the failure of the entire structure. When designing a structure, the maximum buckling capacity is an essential aspect that should be assessed using linear buckling analysis. However, because of manufacturing-induced flaws in the structure itself, the maximum practical load is frequently lower than the expected one. Automating the manufacturing process and installing a robotic filament winding system in the manufacturing facility are two ways to decrease the flaws in a composite material lattice structure [3,4]. Minimising the amount of manual labour is crucial for both lowering manufacturing costs and raising the standard of the final product [5].

Numerous investigations were conducted in the past to comprehend the isogrid structure mechanical behaviour. Yang et al. developed an equivalent continuum model to ascertain the impact strength of lattice structures and validated it by comparing the calculated results with the experimental one [6]. Then, the same model was adopted to examine the behaviour of holed structures. The effect of design parameters was investigated by Kim et al. using an approximation approach [7]. They proposed to explore the buckling of a lattice cylinder made of composite material, investigating both the global and local failure modes. Using a Monte Carlo simulation, Raouf et al. investigated the effects of manufacturing process, geometry, and material uncertainty on the structural properties of an anisogrid lattice structure for the aerospace industry [8]. Kim and Park developed a wing box structure with the aim of minimising weight and examined the impact of various boundary conditions on the buckling performance of a lattice cylinder [9]. The compression strength and energy absorption capacity of aluminium foams were found to be improved by a reinforcement made with a metallic grid as the structural framework, as found by An et al. throughout the production and testing of such components [10]. In order to simulate grid-reinforced panels with fewer computational resources, Akl et al. created a finite element model characterised by a special element [11]. They then utilised this model to examine the efficiency of various rib types, suggesting the superiority of isogrid net over straight one. Swiech used both numerical and experimental methods to investigate the buckling characteristics of an aluminium strengthened plate [12]. He then compared the obtained results to those of a smooth plate of comparable mass and discovered a threefold rise in the first type. In their investigation on how loads and materials affected the structural response of an isogrid structure made of composite material, Lathasree and Yugendher discovered that aramid fibres behaved the best when compared to carbon and glass fibres [13]. Using the Ritz theorem and the shear deformation theory of plates, Ehsani and Dalir evaluated the stability and vibration behaviour of laminated and traditional isogrid structures [14]. They also assessed the impact of the grid geometry and plies count, discovering that the laminated isogrid plate behaved better. In order to investigate the mechanical response of a cylinder with thin walls under a torsional load, Kopecki et al. developed a non-linear numerical model [15]. They then compared the model results with experimental testing and examined the impact of various rib configurations. The process parameters and tools for the production of isogrid structures were identified by Bellini and Sorrentino, who subsequently built and tested some samples [16,17]. These latter stages were crucial for identifying process-induced flaws and streamlining the production procedure. In order to save weight and prevent failure and buckling, Sakata et al. developed a genetic algorithm procedure to create a flawless structural design for a CFRP (Carbon Fiber Reinforced Polymer) isogrid cylinder. By utilising the response surface method as an approximation in place of traditional FEM modelling, the computational time was decreased [18]. By introducing a progressive failure model and comparing the structural properties of laminated lattice structures with those of conventional grid structures, Ehsani and Rezaeepazhand discovered that by carefully choosing the laminated structure stacking sequence, its stiffness could be enhanced without affecting the failure index [19]. A novel method for lowering the amount of computing capacity needed to model the structural characteristics of a cylindrical vessel with isogrid stiffeners was proposed by Hothazie et al. [20]. The vessel was divided into sections, and each component was roughly represented by a thin plate with varied qualities. Sakata and Ben examined the impact of lattice structure on cylindrical shells by implementing a dedicated manufacturing process [21].

The aim of this work is to determine the effect of the material choice on the mechanical capabilities of a stiffened cylinder, which consisted of an exterior thin shell and an isogrid lattice inside. Two materials were considered: CFRP and titanium alloy; therefore, four different structures were examined, as will be illustrated in the materials and methods section. In addition to the mechanical strength performance, the mass of the part was also included in the comparison, since it is an essential parameter in some applications, including those in the automobile and aircraft sectors, in addition to the structural strength qualities [22,23]. To compute the structural behaviour of the isogrid structures, a numerical model was provided. In such a manner, reducing the number of experimental tests was possible, and, consequently, the amount of raw materials and manufacturing resources. Furthermore, since manufacturing-induced faults in the parts would have represented an uncontrollable variable in this study, it was prudent to bypass experimental testing as much as possible. In fact, experiments were taken into consideration only for model validation: the outcomes of the FEM analysis were compared with the experimental tests conducted in earlier work [3].

MATERIALS AND METHODS

The influence of the materials making up the structure on its specific structural properties - that is, its strength to weight ratio and stiffness to weight ratio - was the main focus of this investigation. The numerical model adopted to carry out this analysis was verified on a reference part consisting in an isogrid structure that had been previously designed and experimentally verified [3]. It was composed of ribs supporting a cylindrical skin. The following provides an overview of the design features and the production process; the reader is encouraged to read the previously published article for further details. Using Vasiliev's theory as guidelines, the dimensions of the ribs that constituted the isogrid reinforcement were chosen as 5 mm for the width and 2 mm for the thickness. Unidirectional CFRP, a lightweight material with excellent mechanical properties, was chosen as base material for the isogrid. The other dimensions of this frame were determined as follows: a diameter of 300 mm, a total height of 338 mm, and an overall number of ribs equal to 80, whose five circumferential and the remaining helical. Regarding the skin, FEM simulations were used to establish the laminate thickness, which was determined to be 1.2 mm. The skin was made with carbon fabric, with a thickness of 0.3 mm; therefore, four plies were necessary. As concerns the production of the isogrid structure to be tested, in order to prevent the formation of hazardous strains during the curing process, the epoxy resin mould used in the fabrication of the examined part had a coefficient of thermal expansion that was comparable with that of the composite material. The demountable mould was composed of five components that, when combined, created a cylinder with rib-positioning machined grooves on the outside. Following the assembly and preparation of the mould, the rib material was stratified in the grooves using robotic filament winding technology. This innovative technique involves a robot that is fitted with a particular deposition mechanism for the purpose of laying down the fibre tape, as seen in Fig. 1 (a). Prepregs made of carbon fibres impregnated with epoxy resin were the raw materials that were taken into consideration for the construction of the structure under consideration. To achieve the proper stratification sequence and consistent tape tension, the layering trajectories were precisely determined. Subsequently, the mould was placed on the robot turntable, and the rib material was placed in the grooves. After this phase was finished, the prepreg for the skin was applied to the mould exterior and the ribs. The skin was coated with heat-shrinking tape to provide an adequate amount of consolidation, and the entire package was sealed in a vacuum bag for autoclave curing. When the procedure was complete, the vacuum bag was released, and the mould was extracted away from the part (Fig. 1 (b)). The created isogrid structures underwent a compression test to determine their strength and stiffness. The tests were conducted in a typical dynamometric equipment that had a thick steel plate installed for the structure axial compression. For the compression plate, a displacement at a rate of 1.3 mm/min was chosen.

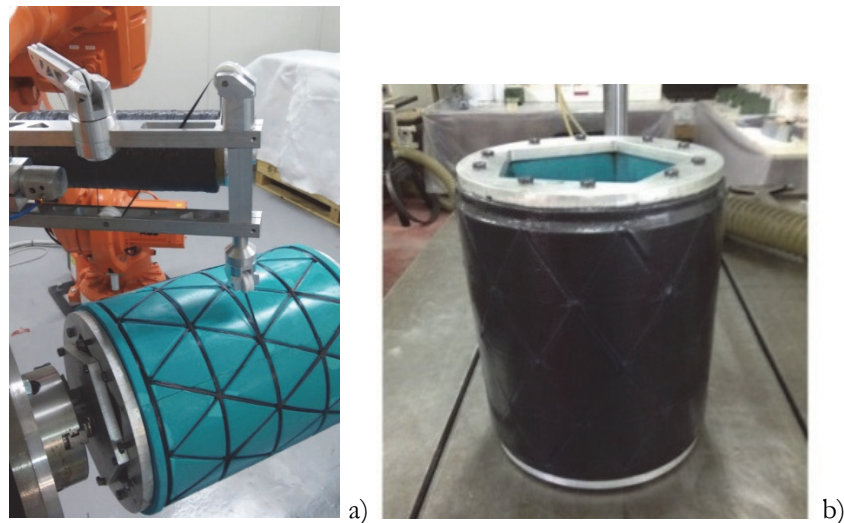


Figure 1: Production of the isogrid structures: (a) tape deposition inside mould grooves; (b) structure before removal of the mould.

A finite element model was presented in the current work to examine the mechanical behaviour of the isogrid structures composed of various materials. Specifically, the strength and stiffness of the entire structure were calculated using the numerical model. As seen in Fig. 2, the mesh utilised for the model includes both the skin and the ribs, which were represented by the shell and beam elements, respectively. There were 24948 nodes, 5860 beam elements, and 21000 shell elements in the implemented model.

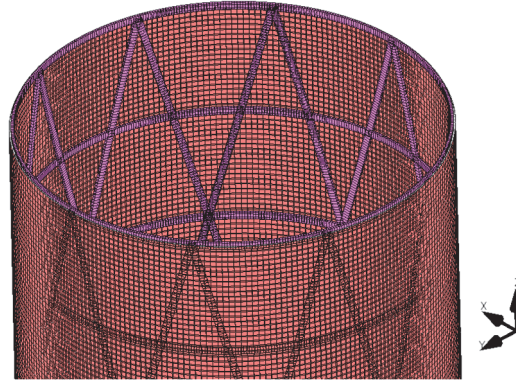


Figure 2: Calculation mesh formed by beam and shell elements.

The computational approach included an elastic linear model, which is defined by a linear connection between stresses and strains. The governing equation is as follows:

$$\sigma_{ij} = C_{ijkl} \epsilon_{kl} \tag{1}$$

where the stiffness matrix is C_{ijkl} , the stress vector is represented by σ_{ij} , and the strain vector is denoted by ϵ_{kl} . The aforementioned equation becomes Hook's law in the case of the titanium alloy because of its isotropic behaviour, but the stiffness matrix for the CFRP material, that is orthotropic, is as follows:

$$C = \frac{1}{(1-\nu_{12}\nu_{21})} \begin{bmatrix} E_1 & \nu_{21}E_1 & 0 \\ \nu_{12}E_2 & E_2 & 0 \\ 0 & 0 & (1-\nu_{12}\nu_{21})G \end{bmatrix} \tag{2}$$

where ν is the Poisson's ratio, G is the shear modulus, and E is the Young's modulus. The damage to the structure at high stress levels was taken into consideration by applying the Hoffman failure criterion. The strength ratio SR was determined by taking the smaller of the absolute values of the two solutions to the given equations:

$$A(SR)^2 + B(SR) + C = 0$$

$$A = \frac{C_1(\sigma_2 - \sigma_3)^2 + C_2(\sigma_3 - \sigma_1)^2 + C_3(\sigma_1 - \sigma_2)^2 + C_7\sigma_{23}^2 + C_8\sigma_{13}^2 + C_9\sigma_{12}^2}{F} \tag{3}$$

$$B = \frac{C_4\sigma_1 + C_5\sigma_2 + C_6\sigma_3}{F}$$

$$C = -1$$

This failure criterion was linked to the deactivation of the element upon failure. The failure index coefficient is denoted by F in the aforementioned equations.

The most common titanium alloy in the aviation industry, Ti6Al4V, was taken into consideration in this study. Regarding the CFRP, it is important to note that a twill fabric was chosen for the skin and a unidirectional prepreg for the ribs. Tabs. 1 and 2 show the material properties of the fabric and unidirectional composite material, respectively, while Tab. 3 reports the titanium material parameters. The boundary conditions were selected considering that the numerical simulation needed to replicate the compression test virtually. In order to recreate the positioning on the testing machine working table, the base of the isogrid cylinder was, therefore, isostatically constrained, and the top of the cylinder was assigned a fixed



compressive displacement to replicate the loading. As shown in Fig. 3, the isostatic constraint was achieved by blocking all the degrees of freedom of one base node and setting to zero the displacement along Z of all base surface nodes, given a reference frame with the Z-axis aligned with the axis of the cylinder. The loading plate was recreated by constraining the translation along -Z of the nodes that belonged to the structure top surface. The loading rate was the same as used for the experimental test. Because the lattice frame was actually glued to the external skin by using a structural adhesive, the ribs were joined to the skin by establishing the coincidences of the nodes.

Mechanical parameter	Value
Tensile strength	276 MPa
Young's modulus	76 GPa
Shear strength	136 MPa
Poisson's ratio	0.3

Table 1: Mechanical parameters of the carbon fabric composite.

Mechanical parameter	Value	Mechanical parameter	Value
Longitudinal strength	1823 MPa	Transversal strength	50 MPa
Longitudinal Young's modulus	213 GPa	Transversal Young's modulus	7.6 GPa
Poisson's ratio	0.28	Shear strength	81 MPa

Table 2: Mechanical parameters of the unidirectional carbon composite.

Mechanical parameter	Value
Tensile strength	880 MPa
Young's modulus	113.8 GPa
Poisson's ratio	0.342

Table 3: Mechanical parameters of the Ti6Al4V titanium alloy.

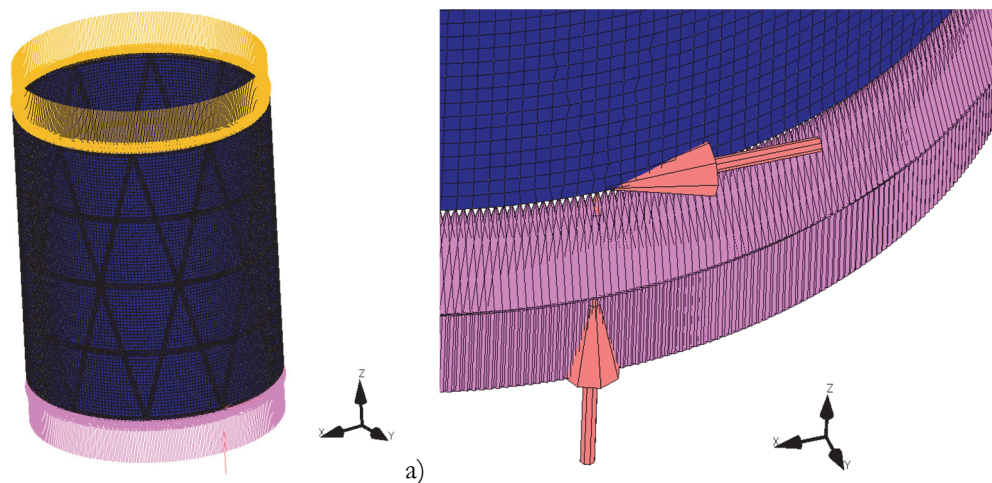


Figure 3: Boundary condition for compression test: (a) constraints on the whole structure (b) node blocked to avoid rigid movements.



The mechanical properties of isogrid parts composed of various materials were examined in the current work; consequently, in order to facilitate a more insightful comparison, the specific mechanical properties - which signify the relationship between a mechanical feature and the weight of the structure - were computed.

RESULTS AND DISCUSSION

This paper presents a finite element model to calculate the properties of an isogrid-stiffened cylinder composed of various materials and to compare their efficiency in terms of performance to weight ratio. Specifically, the mechanical properties of the titanium alloy structure were compared with those of the CFRP one. Moreover, the mechanical properties of hybrid structures, with the stiffener made of CFRP and the skin of titanium, and vice versa, were considered.

Prior to beginning the evaluation, the numerical model that had been provided needed to be validated. For this reason, a CFRP structure simulation was run, and the outcomes were compared to the experimental data that had been previously published in the literature [3]. Fig. 4 presents the findings from both the computational and practical experiments, which are expressed as load-displacement curves. For all five CFRP components that were manufactured and tested, the maximum load gained from the test outcomes was equal to 62.7 kN, with a coefficient of variation of 4.7%, and the stiffness of the structure was equivalent to 540 kN/mm, with a coefficient of variation of 7.8%. It is important to note that the first portion of the curve has a slope that is lower than the value mentioned above, forming a toe region. This effect is frequently observed in experimental results and is caused by slack take-up or specimen seating; for the rigidity calculation, this effect was ignored. The FEM model computed curve showed a linear load increase till 48 kN without a toe like that. Following that point, there were some nonlinearities, and the curve was not completely linear. This continued until the maximum load of 61.0 kN was reached, at which point a drop in load was discovered. In terms of stiffness, the difference was equal to 10.5%, with the predicted rigidity being 483 kN/mm. In terms of maximum load, the difference was 2.7%. It may be inferred from the findings that the created numerical model was appropriate for simulating the structural behaviour of the isogrid structure.

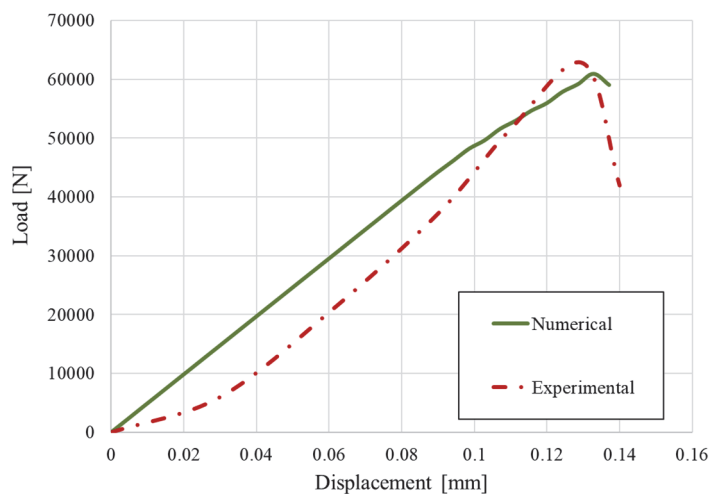


Figure 4: Comparison between numerical and experimental results.

A comparison of the numerical simulation results for all the isogrid stiffened cylinders examined in this work - one composed of titanium only, one of CFRP only, one with CFRP skin and titanium ribs, and the last with CFRP ribs and titanium skin - can be seen in Fig. 5. It can be noted that all the structures presented a similar value of rigidity, which was equal to 483 kN/mm for both the structures with the CFRP ribs, 470 kN/mm for the all-titanium one, and 481 kN/mm for the structure with a titanium lattice and a composite skin. Some discrepancies were found in the maximum load: both the structures with the ribs made of CFRP presented a lower strength compared to those with the ribs made of titanium. In fact, the maximum loads reached by the former ones were 61 kN for the structure with the CFRP skin and 59 kN for that with the titanium skin, while the maximum load of the latter ones was 80.4 kN for the structure with the CFRP skin and 74.5 kN for that with the titanium skin. Based on the previously given findings, it can be deduced that, concerning rigidity, the various isogrid structures exhibited similar values, even if the one combining titanium rib and composite skin had the



highest value. This last type again represented the optimum answer when taking into account the maximum sustainable load, whereas the other structures showed a lesser strength.

Nevertheless, lightness is a crucial factor in aviation applications, thus new considerations about the structures' weight should be made. The density of the titanium alloy was 4430 kg/m^3 , while that of the CFRP was 1480 kg/m^3 for the unidirectional one and 1550 kg/m^3 for the fabric one. Taking into account these densities as well as the geometrical attributes of the structure - all of the structures' dimensions were considered to be the same - the structure composed entirely of CFRP weighed the least at 765 g, while the structure composed entirely of titanium weighed the most at 2212 g. The weights of the other two parts, the titanium skin - CFRP ribs and the CFRP skin - titanium ribs, were 1866 g and 1112 g, respectively. Next, the previously computed maximum load and stiffness were divided by the weight to obtain the specific strength and specific rigidity, respectively. These ratios, which stand for a PI (Performance Index), are frequently used to compare the efficiency of materials, accounting for both their lightweight and mechanical characteristics [24].

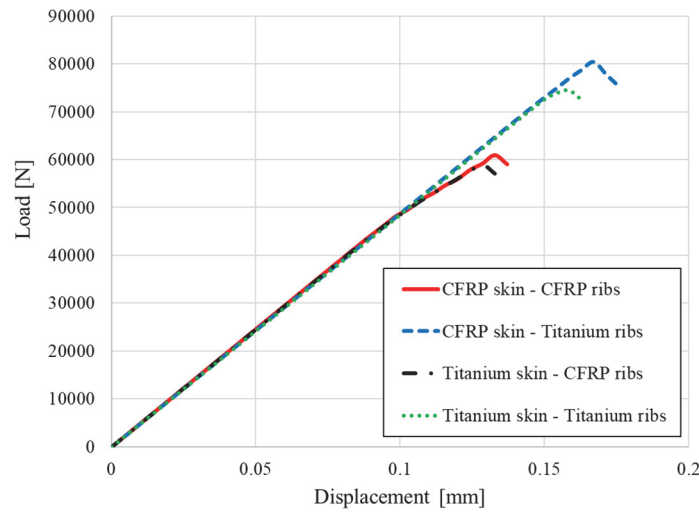


Figure 5: Comparison of the load-displacement curves obtained for the different structures.

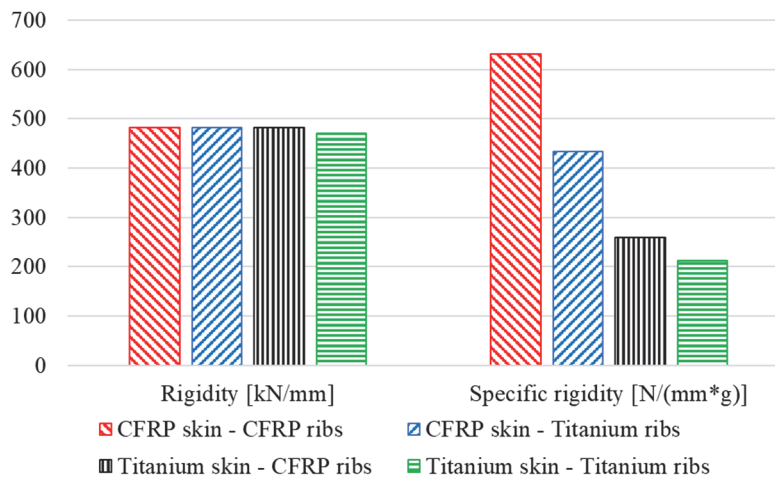


Figure 6: Rigidity comparison for all the studied structures.

As demonstrated by Fig. 6, which examines the stiffness and specific rigidity for each type of isogrid reinforced cylinder, the results of the structural performances previously discussed are altered when weight is taken into account. Actually, the titanium alloy part had the lowest specific rigidity value of $212 \text{ N}/(\text{mm}*\text{g})$, while the CFRP structure showed the best specific rigidity value of $631 \text{ N}/(\text{mm}*\text{g})$. The specific stiffness of the CFRP skin-titanium ribs and the titanium skin-CFRP ribs structures were $433 \text{ N}/(\text{mm}*\text{g})$ and $258 \text{ N}/(\text{mm}*\text{g})$, respectively. The comparison of the strength and the specific strength is visible in the Fig. 7, where the obtained values are reported for all four different kinds of isogrid structure studied in this work. As found for the rigidity, also for the maximum load a certain influence of the weight was detected. In fact, the highest specific strength was reached by the structure made of CFRP only, that arrived at a maximum specific load equal

to 80 N/g, while the lowest value was obtained by that one with the skin made of titanium alloy and the ribs of CFRP, that reached a specific strength of 32 N/g. The all-titanium structure presented a specific strength slightly higher than the latter one; in fact, it was equal to 34 N/g, while the CFRP skin-titanium ribs structure presented a specific strength of 72 N/g. Based on the obtained data, it can be said that weight plays a significant role in the examination of mechanical performances; in fact, it had a significant impact on the mechanical properties themselves. As regards the rigidity, it was found that the proportional variability range, defined as the ratio between the total variability and the average value, was equal to 2.66%. On the contrary, the proportional variability range of the specific rigidity was equal to 108.97%, which means that the maximum obtained value was more than twice the lowest one. As concerns the strength, a higher proportional variability range was found also for the maximum load, which was equal to 31.25%, while this parameter was equal to 88.43% for the specific maximum load. It is therefore possible to draw the conclusion that the constituent material had an impact on some mechanical characteristics, particularly stiffness.

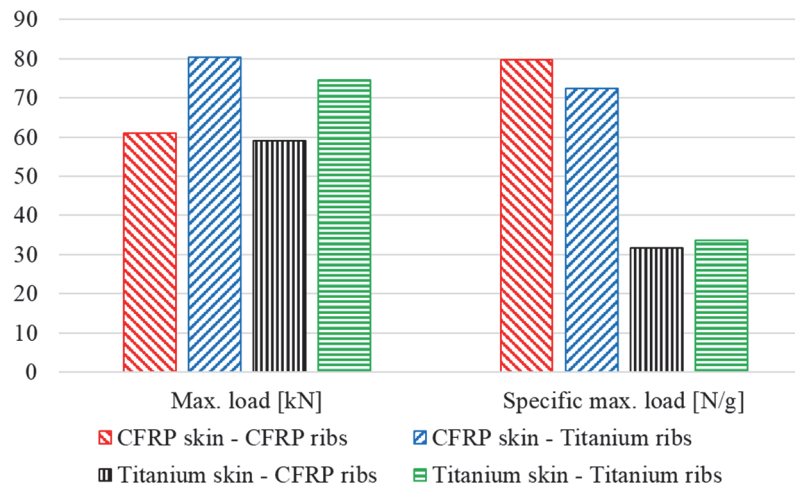


Figure 7: Strength comparison for all the studied structures.

CONCLUSIONS

Due to their ability to achieve high strength-to-weight and stiffness-to-weight ratios through material distribution optimisation, lattice constructions are being used more and more in the manufacture of parts for the aerospace and aviation sectors. The most cutting-edge materials in the aforementioned industry are titanium alloy and composite materials, which are both lightweight and durable. This article compares the structural capabilities of several isogrid structures composed of titanium, CFRP (Carbon Fibre Reinforced Polymer), or a combination of the two materials. Specifically, a numerical simulation was used to determine their structural features; hence, a FEM model was developed and verified for this objective.

The numerical results showed that while there was some fluctuation in strength, stiffness was nearly constant across all structures. Nonetheless, since weight is a crucial factor to take into account for aeronautical applications, the specific structural properties of the various structures - that is, the relationship between the properties and the weight - were ascertained. Numerous intriguing results were discovered when taking these performance indices into account. The CFRP part had the highest specific stiffness, while the all-titanium one had the lowest, with a reduction of 66.3%. The measured reductions for the remaining structures, which consist of titanium skin-CFRP ribs and CFRP skin-titanium ribs, were 59.0% and 31.3%, respectively. In terms of the specific strength, the CFRP structure likewise produced the best results for this metric, while the titanium skin-CFRP ribs were the worst ones, with a reduction of 60.3%. The other structures, that were the CFRP skin - titanium ribs and the titanium-only, showed a reduction of 9.1% and 57.7%, respectively.

The results of this study demonstrate the advantages of composite lattice structures over metal ones in terms of structural specific characteristics. The former can be employed in aerospace and aviation applications where high stiffness and strength are necessary in addition to structure lightness. However, hybrid structures, made with different materials, present interesting specific characteristics too.



REFERENCES

- [1] Forcellese, A., Simoncini, M., Vita, A., Di Pompeo, V. (2020). 3D printing and testing of composite isogrid structures, *Int. J. Adv. Manuf. Technol.*, 109(7–8), pp. 1881–1893, DOI: 10.1007/s00170-020-05770-4.
- [2] Giusto, G., Spena, P., Totaro, G., de Nicola, F., Di Caprio, F., Zallo, A., Cioeta, M., Mespoulet, S. (2018). Interstage 2-3 of Vega C launcher: Composite grid structure technology. *ECCM 18-18th European Conference on Composite Materials*.
- [3] Sorrentino, L., Marchetti, M., Bellini, C., Delfini, A., Del Sette, F. (2017). Manufacture of high performance isogrid structure by Robotic Filament Winding, *Compos. Struct.*, 164, pp. 43–50, DOI: 10.1016/j.compstruct.2016.12.061.
- [4] Sorrentino, L., Anamateros, E., Bellini, C., Carrino, L., Corcione, G., Leone, A., Paris, G. (2019). Robotic filament winding: An innovative technology to manufacture complex shape structural parts, *Compos. Struct.*, 220(March), pp. 699–707, DOI: 10.1016/j.compstruct.2019.04.055.
- [5] Sorrentino, L., Bellini, C. (2016). Potentiality of Hot Drape Forming to produce complex shape parts in composite material, *Int. J. Adv. Manuf. Technol.*, 85(5–8), pp. 945–954, DOI: 10.1007/s00170-015-7998-x.
- [6] Yang, Q., Yang, S., Lin, X. (2015). Impact response of stiffened cylindrical shells with/without holes based on equivalent model of isogrid structures, *Comput. Mater. Contin.*, 45(1), pp. 57–74, DOI: 10.3970/cmc.2015.045.057.
- [7] Kim, Y., Kim, P., Kim, H., Park, J. (2019). An optimization of composite lattice cylinder using the approximate method, *Adv. Compos. Mater.*, 28(3), pp. 287–320, DOI: 10.1080/09243046.2018.1510590.
- [8] Raouf, N., Davar, A., Pourtakdoust, S.H. (2022). Reliability analysis of composite anisogrid lattice interstage structure, *Mech. Based Des. Struct. Mach.*, 50(9), pp. 3322–3330, DOI: 10.1080/15397734.2020.1822180.
- [9] Kim, Y., Park, J. (2020). An approximate approach on the buckling analysis of a composite lattice cylindrical panel, *Adv. Compos. Mater.*, 29(6), pp. 603–630, DOI: 10.1080/09243046.2020.1755100.
- [10] An, Y., Yang, S., Zhao, E., Wang, Z. (2018). Fabrication and experimental investigation of metal grid structure-reinforced aluminum foams, *Mater. Manuf. Process.*, 33(5), pp. 528–533, DOI: 10.1080/10426914.2017.1364747.
- [11] Akl, W., El-Sabbagh, A., Baz, A. (2008). Finite element modeling of plates with arbitrary oriented isogrid stiffeners, *Mech. Adv. Mater. Struct.*, 15(2), pp. 130–141, DOI: 10.1080/15376490701810472.
- [12] Świech, L. (2019). Experimental and numerical studies of low-profile, triangular grid-striated plates subjected to shear load in the post-critical states of deformation, *Materials (Basel)*, 12(22), DOI: 10.3390/ma12223699.
- [13] Lathasree, P., Yugendher, M. (2019). Design and optimization of an isogrid composite cylinder using FEA, *Int. J. Mech. Prod. Eng. Res. Dev.*, 9(6), pp. 463–474, DOI: 10.24247/ijmperdec201940.
- [14] Ehsani, A., Dalir, H. (2019). Influence of employing laminated isogrid configuration on mechanical behavior of grid structures, *J. Reinf. Plast. Compos.*, 38(16), pp. 777–785, DOI: 10.1177/0731684419848046.
- [15] Kopecki, T., Mazurek, P., Lis, T. (2019). Experimental and numerical analysis of a composite thin-walled cylindrical structures with different variants of stiffeners, subjected to torsion, *Materials (Basel)*, 12(19), DOI: 10.3390/ma12193230.
- [16] Bellini, C., Sorrentino, L. (2018). Mould design for manufacturing of isogrid structures in composite material, *Procedia Struct. Integr.*, 9, pp. 172–178, DOI: 10.1016/j.prostr.2018.06.027.
- [17] Bellini, C., Sorrentino, L. (2018). Characterization of Isogrid Structure in GFRP, *Frat. Ed Integrità Strutt.*, 46, pp. 319–331, DOI: 10.3221/IGF-ESIS.46.29.
- [18] Sakata, K., Suzuki, T., Ben, G. (2018). Optimum structural design of CFRP isogrid cylindrical shell using genetic algorithm, *Adv. Compos. Mater.*, 27(1), pp. 35–51, DOI: 10.1080/09243046.2017.1342063.
- [19] Ehsani, A., Rezaeepazhand, J. (2017). Comparison of stiffness and failure behavior of the laminated grid and orthogrid plates, *J. Solid Mech.*, 9(1), pp. 126–137.
- [20] Hothazie, S., Munteanu, C., Nastase, M., Bibire, R. (2018). Analysis of isogrid reinforced cylindrical vessels in the case of axially symmetric buckling, *INCAS Bull.*, 10(3), pp. 89–101, DOI: 10.13111/2066-8201.2018.10.3.8.
- [21] Sakata, K., Ben, G. (2012). Fabrication method and compressive properties of CFRP isogrid cylindrical shells, *Adv. Compos. Mater.*, 21(5–6), pp. 445–457, DOI: 10.1080/09243046.2012.743711.
- [22] Figlus, T., Koziol, M., Kuczyński, Ł. (2019). Impact of application of selected composite materials on the weight and vibroactivity of the upper gearbox housing, *Materials (Basel)*, 12(16), 2517, DOI: 10.3390/ma12162517.
- [23] Shevtsov, S., Zhilyaev, I., Oganessian, P., Axenov, V. (2016). Material distribution optimization for the shell aircraft composite structure, *Curved Layer. Struct.*, 3(1), pp. 214–222, DOI: 10.1515/cls-2016-0017.
- [24] Sorrentino, L., Bellini, C., Polini, W., Turchetta, S. (2018). Performance Index of Natural Stones-GFRP Hybrid Structures, *Frat. Ed Integrità Strutt.*, 46, pp. 285–294, DOI: 10.3221/IGF-ESIS.46.26.